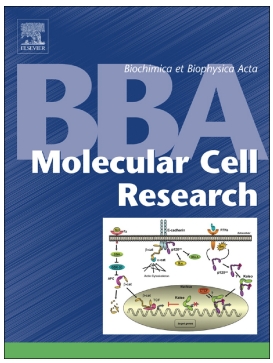


# Decrease of Rab11 prevents the correct dendritic arborization, synaptic plasticity and spatial memory formation

Sebastian O. Siri, Victoria Rozés-Salvador, Emilce Artur de la Villarmois, Marisa S. Ghersi, Gonzalo Quassollo, Mariela F. Pérez, Cecilia Conde

PII: S0167-4889(20)30093-8

DOI: https://doi.org/10.1016/j.bbamcr.2020.118735

Reference: BBAMCR 118735

To appear in: *BBA - Molecular Cell Research*

Received date: 3 February 2020

Revised date: 27 April 2020

Accepted date: 2 May 2020

Please cite this article as: S.O. Siri, V. Rozés-Salvador, E.A. de la Villarmois, et al., Decrease of Rab11 prevents the correct dendritic arborization, synaptic plasticity and spatial memory formation, *BBA - Molecular Cell Research* (2020), https://doi.org/10.1016/j.bbamcr.2020.118735

# Decrease of Rab11 prevents the correct dendritic arborization, synaptic plasticity and spatial memory formation

Sebastian O Siri[1-2a], Victoria Rozés-Salvador[1-3a], Emilce Artur de la Villarmois[4], Marisa S. Ghersi[4], Gonzalo Quassollo[1-2], Mariela F. Pérez[4], Cecilia Conde[1-2 *]

1. Universidad Nacional de Córdoba (UNC) Av. Haya de la Torre s/n Ciudad Universitaria, 5000, Córdoba, Argentina

2. Instituto de Investigación Médica Mercedes y Martıín Ferreyra (INIMEC-CONICET) Av. Friuli 2434, 5016, Córdoba, Argentina

3. Instituto A.P. de Ciencias Básicas y Aplicadas, Universidad Nacional de Villa María (UNVM), Arturo Jauretche 1555, Ciudad Universitaria, Villa María, Argentina

4. IFEC, CONICET, Departamento de Farmacologia, Facultad de Ciencias Químicas, UNC, Haya de la Torre Y Medina Allende, 5000, Córdoba, Argentina

* **Corresponding author**: Cecilia Conde
Instituto de Investigación Médica Mercedes y Martín Ferreyra (INIMEC-CONICET)
Av. Friuli 2434, 5016, Córdoba, Argentina
+5435194681465 (ext 133)
E-mail: cconde@immf.uncor.edu (CC)

[a]These authors contributed equally to this work and should be considered as first authors.

**Abstract**

Emerging evidence shows that Rab11 recycling endosomes (REs Rab11) are essential for several neuronal processes, including the proper functioning of growth cones, synapse architecture regulation and neuronal migration. However, several aspects of REs Rab11 remain unclear, such as its sub-cellular distribution across neuronal development, contribution to dendritic tree organization and its consequences in memory formation. In this work we show a spatio-temporal correlation between the endogenous localization of REs Rab11 and developmental stage of neurons. Furthermore, Rab11-suppressed neurons showed an increase on dendritic branching (without altering total dendritic length) and misdistribution of dendritic proteins in cultured neurons. In addition, suppression of Rab11 in adult rat brains *in vivo* (by expressing shRab11 through lentiviral infection), showed a decrease on both the sensitivity to induce long-term potentiation and hippocampal-dependent memory acquisition. Taken together, our results suggest that REs Rab11 expression is required for a proper dendritic architecture and branching, controlling key aspects of synaptic plasticity and spatial memory formation.

**Keywords**

Synaptic plasticity - Rab11- Spatial memory- Neuronal development- Recycling endosomes

**Abbreviations**

REs, recycling endosomes; TfR, transferrin receptor; mGluR1, metabotropic glutamate receptor 1; LTP, long-term potentiation; VAMP2, vesicle-associated membrane protein 2; DIV, days *in vitro*; PI, polarity index; sCFC, standard Contextual Fear Conditioning; OF, open field; CS, conditioned stimulus

## 1. Introduction

The mammalian Rab proteins belong to the Ras superfamily of small GTPases, being evolutionarily conserved and critical regulators of vesicle trafficking and sorting proteins to their target membranes [1-3]. Sub-cellular localization of the Rabs contributes to identifying the endosomal membrane source, allowing cargoes reaching suitable domains in the cell [4, 5]. Rabs also have multiple protein-binding domains, allowing interactions with regulatory and effector molecules, participating in a large number of activities in polarized and non-polarized cells [6-9]. Rab11 is one of the best characterized recycling endosomes (REs) marker, able to regulate the slow recycling pathway [10, 11], and critical for differential recycling of membrane proteins, receptors and lipids of plasma membrane [7, 12].

Neurons represent one of the most polarized cells in nature, displaying several short and thick conical dendrites and one functional thin axon [13, 14]. Accordingly, diverse membrane proteins are segregated to dendrites and/or the axon through different mechanisms [15-17]; therefore, defects in either protein localization or trafficking are associated with a wide variety of neuronal diseases, like autism spectrum disorders, Alzheimer's and Huntington's disease, linking REs dynamics with neurological disorders [18, 19].

During neuronal development, Rab11 participates in the initiation, maintenance, and regulation of different processes [20]. Specifically, Rab11 is involved in the regulation of AMPA receptor recycling in dendrites [21, 22] as well as in axonal trafficking of Trk receptors [23]. Furthermore, Rab11 participates in axonal growth; overexpression of Rab11 increases axonal growth, whereas reduction of Rab11 decreases axonal length of cortical neurons [24]. Similar results were obtained in dorsal root ganglia and PC12 cells [25]. Accordingly, the expression of constitutively active forms of Rab11 increases dendritic branching in hippocampal neurons; however, no effects on branching were observed after Rab11 loss of function either by dominant negative mutants or shRNA expression [26]. Moreover, Rab11 is needed for the intrinsic regenerative capacity of the axons (after axotomy) of mouse cortical neurons [27]. Recently, the Cdk5–LMTK1–TBC1D9B–Rab11A cascade was proposed as a novel signaling axis controlling the physiology of dendritic spines [28]. Finally, *in vivo* experiments have proposed that Rab11 is key for neuronal migration and maturation during mouse corticogenesis; accordingly, trafficking of N-Cadherin to the plasma membrane occurs through Rab11-dependent recycling pathways [29].

Previous studies have reported the role of Rab11 in axon elongation, neuronal migration and spines remodeling. Nevertheless, its contribution to dendritic growth and branching required for proper synaptic transmission has remained unexplored. Therefore, in this work we analyze sub-cellular distribution of REs Rab11 throughout neuronal development and somatodendritic protein localization, describing the consequences of suppressing Rab11 on dendritic growth, arborization and synaptic transmission.

Our results suggest a dynamic distribution of REs Rab11 according to the different stage of neuronal development. Rab11 suppression missdistributed the transferrin receptor (TfR) and the metabotropic glutamate receptor (mGluR1), two dendritic

membrane proteins, modifying dendritic branching. Furthermore, *in vivo* suppression of Rab11 altered the long-term potentiation (LTP) response, an experimental paradigm to evaluate synaptic transmission and memory acquisition. Collectively, our work suggests a functional link between dendritic growth, branching and neural activity mediated by Rab11.

## 2. Materials and Methods

### *2.1 Antibodies*

Primary antibodies: Anti-Tau (clone Tau-1) and anti-MAP2 (clone AP-18) proteins were used as axonal and dendritic markers, respectively (a generous gift of Dr. L. I. Binder, Northwestern University, Chicago, USA) and were diluted 1:1,500 and 1:400, respectively. Anti-tyrosinated α-tubulin (Tyr-Tubulin; Sigma Ch. Co. USA) was diluted 1:10,000; anti-Rab11 (sc- 9135, Santa Cruz Biotechnology, Inc. CA, USA) was diluted 1:50 for IF or 1:200 for WB; anti-Myc (sc-789, Santa Cruz Biotechnology, Inc. CA, USA) was diluted 1:400; anti-Flag (Sigma Aldrich) was diluted 1:500; Rhodamine-Phalloidin (Molecular Probes, Eugene, OR, USA) was diluted 1:1,000. Secondary antibodies conjugated with: Alexa 488 (Molecular Probes, Thermo Fisher Scientific Cat #: A11029 and A11006, dilution 1:1000), and/or Alexa 568 (Molecular Probes, Thermo Fisher Scientific; Cat #: A11077 and A11004, dilution 1:1000) and/or Rhodamine Phalloidin (Molecular Probes Invitrogen, Lot: 355-45A, dilution 1:500).

### *2.2 DNA constructs*

TfR-GFP and VAMP2-GFP were provided by Dr. A. Gonzalez (Universidad Catolica Chile, Santiago, Chile) and Dr. Thierry Galli (Inserm, Institut Jacob Monod, Paris, France) and mGluR1-Myc was a contribution from Dr. G. Banker. The mCherry

constructions were obtained by replacing the EGFP with mCherry using AgeI/BsrGI restriction enzymes. The short hairpin RNA forRab11a-untagged (shRab11-1) was kindly provided by Dr. Kawauchi (Department of Anatomy, Keio University School of Medicine, Tokyo 160-8582, Japan;) and shRab11-2 by Dr. Esteves da Silva (Cell Biology, Faculty of Science, Utrecht University, 3584 CH Utrecht, the Netherlands). As targeting sequences were: 5'-GCATCCAGGTTGATGGGAA-3' (for shRab11-1; [29]), and 5′-GTACGACTACCTCTTTAAA-3′ (for shRab11-2; [22]). These sequences were subcloned into pBS/U6 vector following the procedures described by [17]. Scrambled control shRNA plasmid (shSc) was purchased from Ambion Co.

### *2.3 Primary culture of hippocampal neurons*

Pregnant Wistar rats were sacrificed and both female and male embryos (embryo day 18, E18) were removed to isolate hippocampal neurons for culture as previously described [30]. All experiments were approved by the Bioethical Research Committee of INIMEC-CONICET-UNC and conducted following the guidelines of by the animal care and use committee of Instituto Ferreyra (INIMEC-National Research Council and Universidad Nacional de Córdoba, Argentina), the National Department of Animal Care and Health (SENASA-Argentina).

### *2.4 Transient electroporation*

Neurons were electroporated before plating with the plasmids encoding cDNAs using the Amaxa Nucleofector II device (Lonza, Cat Number: AAD-1001N), following manufacturer's instructions and program O-003 for Primary Rat Hippocampal Neurons. Three days after electroporation the neurons were fixed.

### *2.5 Lentivirus particles production*

HEK-293T cells were plated into a 10 cm culture dish up to a density of 25%. Cells at 80-90% of confluence were transfected with plasmids encoding both envelope and capsid proteins (pVSVg (4, 5μg); pREV (4, 5μg); p8.74 (9μg)) and the pLentiLox 3.7 vector (10μg) [31] carrying the shRab11 sequence using Lipofectamine. Medium was replaced after 3h (DMEM-10% Fetal Bovine Serum-1% Glutamax and 1% Pen/Strep). After 48-72h, the supernatants were collected and centrifuged at 12,000 rpm for 10 min. Then were filtered at a 0.45 μm pore size, centrifuged at 13,000 rpm for 2h at 4°C; then, pellet was resuspended in saline solution.

### *2.6 Immunofluorescence*

Cells were fixed (20 min) with 4% (w/v) paraformaldehyde (Sigma, Aldrich; Cat Number: 441244) containing 4% (w/v) sucrose (Anedra; Cat Number: AN00711809) and permeabilized for 5 min with 0.2% (v/v) Triton X-100 (Bio-Rad Laboratories, Hercules, CA, USA; Cat Number: 1610407). After fixation, cells were incubated (1h) in blocking buffer (5% bovine serum albumin in PBS). Primary and secondary antibody incubations were carried out in buffer containing 1% bovine serum albumin in PBS during 1h and mounted using Mowiol (Sigma Aldrich). Imaging quantification were performed using Fiji-ImageJ software [32, 33], pixel by pixel and data were used to calculate the average fluorescence intensity expressed in pixels (0= black /255= white). Cells were visualized using either a spectral (Olympus Fluoview1000) or LSM 800 (Zeiss) (Lasers: 488, 533 and 633; resolution X=1024; Y=1024 and Z=0.3-0.5 μm; Objectives: 63X: Plan-Apochromat 63X/1.40 Oil DICM27 and 20X: Objective 20X LD Apochromat 20X/0.40, both inverted confocal microscopes.

### *2.7 Morphometric analysis*

Confocal images of neurons were processed using a Fiji-ImageJ software macro. Macro commands were applied to the selection area to remove the background outside that area. After image processing, Sholl analysis was performed to quantify dendritic arborization (Sholl analysis v3.4.10 plugin for ImageJ [34]). For measurements, a straight line was traced from the center of the cell body to the end of the neurites; intersections were analyzed from an initial radius of 10 µm to the maximum radius in steps of 5 µm. The order of the branches was quantified manually, considering the primary order to the first branch, and emerging branches that come from it, as secondary. Tertiary and quaternary order branches were defined following same criteria. Neurons with more than 4 neurites were included in this analysis. Neurites with a strong Tau-1 signal at their proximal end were counted as axons.

Morphological quantification of dendritic spines was performed manually as previously described [35]. Extensions of more than 4 microns were classified as filopodia. The spines were counted only if they were continuous with the original dendrite. Column density was calculated by quantifying the number of spines (labeled with GFP) per dendritic segment and normalized to 20 µm dendrite length.

The duration and number of processes were quantified as previously described [36]. The quantification of the polarity index to analyze the somatodendritic or axonal distribution of the receptors was performed as described [17].

### *2.8 Stereotaxic injections*

Two-month-old male rats (250-280 kg) were anesthetized with ketamine/xylazine mixture (100 mg/kg and 10 mg/kg respectively) and were injected stereotaxically by Kopf stereotaxic apparatus (Tujunga, California, USA) with equal amounts of lentiviral particles as expressing Scramble-GFP or shRab11-GFP (3 µl in continuous flow of 6 ml

/ min) in the CA1 region of the dorsal hippocampus (from Bregma: AP: 3.3; L: 2.0; and V: 2.9). The injections were performed unilaterally and after 7 min the cannula was removed. Later the animal was placed in a box on a thermal blanket for recovery.

### *2.9 Slice electrophysiology*

Rats were sacrificed by guillotine decapitation 7 days after the stereotaxis between 10:00 and 11:00 am, to prevent variations caused by circadian rhythms or nonspecific stressors [37]. Electrophysiological experiments were performing using the *in vitro* HP slice preparation [38]. Briefly, the hippocampus was removed and 400 μm cross slices were made and kept in a storage chamber containing Krebs standard solution (NaCl, 124.3 mM; KCl, 4.9 mM; $MgSO_4 \cdot 7H_2O$, 1.3mM; $H_2KPO_4$, 1.25 mM; $HNaCO_3$, 25.6 mM; glucose, 10.4 mM; $CaCl_2 \cdot 2H_2O$, 2.3 mM; Sigma) saturated with 95% $O_2$ and 5% $CO_2$. For analysis, the slices were placed in a recording chamber (Harvard BSC-BU Apparatus) perfused with the Krebs standard solution (1.6 ml/min, at 28° C). The postsynaptic field excitatory potentials (EPSP) were evoked by an A310 acupulsor pulse generator (World Precision Instruments Inc.) with a stimulating electrode consisting of two wires, which were isolated except for the cut ends (diameter 50 μm) of the perforated path (PP). Then, a recording microelectrode was inserted into the body layer of toothed granular cells. Only the slices that showed a stable response were included in the study. EPSP was evoked by a basal square pulse train (40 V, 0.5 ms each) at 0.2 Hz and samples were taken every 5 min, for 40 min until EPSP stabilization (baseline). Once the EPSP amplitude stabilized, one of the two stimulation protocols was performed. In the first protocol (high-frequency pacing, HFS), LTP was generated using the classic tetanization paradigm consisting of three 100-Hz high-frequency pacing trains (1 s each) administered at 20 s intervals. In the second protocol applied, the

stimulation allowed us to assay different stimulating frequency values in order to determine the minimum value to generate LTP (we call this "threshold" value). The stimulus consisted of a train of square pulses 2 s in length, with 0.5 ms being the duration of each square pulse. We used different stimulus frequencies in each segment at 20 Hz intervals, starting at 20 Hz to 200 Hz. For both protocols, LTP was considered to occur when the amplitude of EPSP recorded after the stimulus had increased by at least 30% from the start and persisted for 60 minutes. Once LTP was generated, EPSP amplitude was recorded every 20 minutes to record the LTP time profile (maintenance and magnitude after the stimulation protocol). The results were expressed as a percentage of the change in EPSP amplitude related to the baseline ± SEM and were analyzed by prior calculation of repeated measures bidirectional ANOVA from Fisher's exact test (F). For the analysis of both protocols, the level of significance was established at $\alpha = 0.05$ and the post-Holm-Sidak multiple comparisons test were used.

### *2.10 Behavioral analysis*

Six days after the stereotaxic procedure, the animals were subjected to several behavioral tests: locomotor activity was analyzed in an open field (OF), and a standard contextual fear conditioning test (sCFC) was carried out for the rearing and freezing activity [39]. This sCFC test consists of placing the animal in a fear-conditioned plexiglass camera (40 x 36 x 31 cm, W, L, H) with a base grid, containing different visual signals (black and white stripes on the wall) and with vanilla essence as olfactory key (conditioned stimulus, CS). On the training day, the animal is placed inside the chamber and recorded in this context for 5 minutes. After 4 minutes, the animal receives a 0.50 mA shock for 2 seconds and the remaining minute is left in the chamber. Subsequently, the animal is removed and left in its starting box until the next day. On

the day of the test, the animal is placed back into the chamber and the animals' behavior was video recorded under the same contextual cues. Using a time sampling procedure every 2 s, each animal was blindly classified as freezing or active at the time the sample was taken. Freezing was defined as behavioral immobility except the movement necessary for breathing. All experiments were performed between 8:30 a.m. and at 15:00 p.m.

### *2.11 Statistics*

All data are shown as mean ± SEM. Statistical analyses were performed by Student's *t* test or one-way ANOVA or repeated measures one-way ANOVA for comparisons among three or more conditions. The significance was reported as $p < 0.05$ *, $p < 0.01$ ** and $p < 0.001$ ***. Normality of the variables was tested by the Shapiro-Wilks test. Statistical significance was set at $*p < 0.05$. Analyses were performed using the free programming language R (https://www.rstudio.com/; R Development Core Team, 2008).

For behavior experiments, two-way repeated-measures ANOVA were used with Post-Hoc Hold Sidak correction to test significance.

## 3.Results

### *3.1 Distribution and sub-cellular localization of REs Rab11 during neuronal development*

The expression of REs Rab11in polarized cells has been mainly described in cell lines (PC12, MDCK and epithelial cells) [6, 7, 12]. Previous reports in neurons show that the location of the REs Rab11 has been analyzed at fixed culture time, and particularly focused on the study of axonal or dendritic receptors trafficking associated with these REs [21-23]. However, detailed analysis of REs localization throughout neural development is missing. Therefore, we analyzed the endogenous distribution of REs Rab11 in neurons cultured for1, 3, 7, 14 and 21 days *in vitro* (DIV) by immunofluorescence (IF) using a specific antibody against Rab11 (Fig. 1). We found that REs Rab11 distribute throughout the entire soma (clustered closely from the nucleus, neighbouring the trans-Golgi network) and neurites in all culture times analyzed in this study (Fig. 1A-J). Furthermore, at 1 DIV, REs Rab11 were not uniformly distributed across neurites, being mainly enriched at neurite tips (Fig. 1A-A') and central domains of growth cones (Fig. 1B). In contrast, after 3 DIV, endosomal distribution was uniform throughout the neuritic processes (Fig. 1C, C', D), while REs Rab11 were enriched towards the proximal region of neurites after 7 and 14 DIV (Fig. 1E, E', F and G, G', H, respectively). Finally, at 21 DIV (when dendritic tree is fully developed and neurons already mature for synaptic transmission), REs Rab11 were uniformly distributed throughout the processes (Fig. 1I, I', J). Quantification of Rab11-positive puncta in neuritic processes revealed an increase in the number of REs Rab11 in the proximal region at 7 and 14 DIV neurons (Fig. 1K); in contrast, 1 DIV neurons showed that these endosomes are mainly located in neuritic tips (distal region in Fig. 1L). Together, these results suggest a segregated distribution of REs Rab11 in neuritic

processes of cultured neurons, which seems to be a requirement at different stages of development to achieve the demands of the neuron, associated to growing and maturation.

### *3.2 Rab11 suppression changes the morphology of the dendritic tree*

Previous reports have shown the contribution of other members of Rab-GTPases, to dendritic and axonal morphology; Rab10 promotes axon elongation and dendritic branching in *C. elegans* sensory neurons [40, 41], whereas Rab5 and Rab4 regulate axon elongation in retinal ganglion cells of *X. laevis* [42]. Therefore, we evaluated the consequences of Rab11 suppression during neuritic morphogenesis to unveil REs Rab11 contribution to dendritic arborization and neuronal activity. Accordingly, cultured hippocampal neurons were electroporated before plating (t=0) with two specific shRNAs to suppress endogenous Rab11 (shRab11-1 and -2); shScramble (shSc) was used as control. Knock-down efficiencies of shRab11-1 and shRab11-2 were measured by Western Blot, reaching 57% and 51% of Rab11 reduction for shRab11-1 and shRab11-2, respectively (Supplementary Fig. S1A-B). Morphologically, we found that Rab11-suppressed neurons of 3 and 7 DIV showed more complex dendritic trees than controls (Fig. 2A-B). Of note, and based on the fact that both shRNAs used in this study reported similar knock-down efficiencies and same phenotype, the following data represents experiments assayed with shRab11-1 (called "shRab11"from this point forward). Using a Sholl analysis, we quantified dendritic branching in electroporated neurons; accordingly, Rab11-suppressed neurons showed a higher number of intersections between dendrites compared to control neurons at 3 and 7 DIV (Fig. 2C, E), suggesting a more complex dendritic arborization after Rab11 suppression. In addition, the average branching order in both experimental and control groups was

quantified, being consistent with the increase in the number of branching points observed in Rab11-suppressed neurons in primary, secondary, tertiary and quaternary dendrites at 3 and 7 DIV (Fig. 2D, F). In addition, we observed an increase in the number of primary processes (directly emerged from the soma) in Rab11-suppressed neurons at 3 DIV, which was not observed at 7 DIV (Fig. 2G). We also observed a decrease in the total neurite length in Rab11-suppressed neurons at 3 DIV, but this was not observed at 7 DIV (Fig 2H). However, at 3 DIV the average of total length of dendritic tree in electroporated cells was ~425 μm for both conditions (430±25 μm and 420±21.5 μm, shSc and shRab11 respectively; p= 0.08). Of note, the same tendency was observed in cells after 7 DIV (831±40.77μm and 845±32.63μm, shSc and shRab11 respectively; p= 0.786). Together, our results suggest that REs Rab11 participate not only in dendritic spines morphogenesis, but also in the proper development and branching of the dendritic tree of developing neurons.

### *3.3 Rab11 suppression modifies the intracellular distribution of dendritic proteins*

It is widely accepted that neuritic growth and complexity depends on protein and lipids supply, a phenomenon mostly mediated by Rabs-dependent membrane trafficking [20, 43-47]. Therefore, we evaluated the intracellular distribution of receptors transported by REsRab11 in neuronal compartments, since this could explain the increase on dendritic branching observed in Rab11-suppressed neurons. Accordingly, we analyzed the distribution of membrane proteins, such as transferrin receptor (TfR) and metabotropic glutamate receptor 1 (mGluR1), in Rab11-suppressed neurons at 3 and 7 DIV [48, 49]. Consistently with previous reports, confocal images of control neurons (co-transfected with shSc-GFP and TfR-mCherry) showed an enrichment of TfR in the somatodendritic domain (defined by MAP2 staining) in discrete vesicles or tubulo-vesicular organelles,

some of which were neighbouring the plasma membrane (Fig. 3A) [50]. In contrast, co-transfected neurons with shRab11-GFP and TfR-mCherry revealed that TfR was found not only in dendrites (MAP2-positive) but also in axons (MAP2-negative) (Fig. 3B).

Similar results were obtained in neurons co-transfected with either shRab11-GFP or shSc-GFP and mGluR1-myc. Control neurons showed a vesicle-pattern localization for mGluR1, mostly distributed throughout the cell body as well as in Tau1-negative processes (Fig. 3C). However, in Rab11-suppressed neurons, the expression of mGluR1 showed an enrichment in the axonal domain (Tau1-positive) (Fig. 3D). As a negative control we analyzed the distribution of the vesicle-associated membrane protein 2 (VAMP2), which is transported through a Rab11-independent mechanism [51]. Accordingly, confocal images of co-transfected neurons with shRab11-GFPor shSc-GFP and VAMP2-mCherry showed that VAMP2 is localized in the axonal and somatodendritic domain in both Rab11 suppressed and control neurons (Fig. 3E-F).

Changes in the localization of TfR, mGluR1 or VAMP2 were quantified using a "polarity index" (PI) described in previous studies [17, 52, 53]. Briefly, the average of the fluorescence intensity in dendrites was divided by the axonal intensity of proteins analyzed; this ratio was defined as PI. Of note, PI values close to 1 report uniform distribution between axonal and dendritic domains, whereas PI values above and below 1 suggest dendritic and axonal enrichment, respectively. Control neurons showed higher PI for TfR in relation to those transfected with shRab11-GFP (PI 1.46 vs 1.09 to 3 DIV and 1.45 vs 0.8 to 7 DIV neurons; Fig. 3G-H, respectively). Similar results were detected for mGluR1, since control neurons showed a significantly higher PI than Rab11-suppressed neurons (PI 1.65 vs 1.10, to 3 DIV and 1.42 vs 1.04 to 7 DIV neurons; Fig. 3G-H respectively). Thus, PI estimation revealed that suppressingRab11 induces TfR and mGluR1 missorting. Finally, as expected, VAMP2 showed an

unpolarized distribution at 3 and 7 DIV, since it was found in both axonal and somatodendritic domains (Fig. 3G-H). Collectively, these results suggest that increased dendritic branching after Rab11 suppression also changes the specific delivery of membrane proteins (as TfR and mGluR1) to the somatodendritic domain.

### *3.4 The loss of function of Rab11 reduced the sensitivity to induce long-term potentiation (LTP) in the hippocampal dentate gyrus*

To analyze the effect of Rab11 suppression *in vivo*, we performed stereotaxic surgery, injecting animals with lentiviral particles carrying shRab11or shSc in the CA1 brain region of adult rats. Histological sections (40 μm) were used; in which infection efficiency was mainly observed in the *dentate gyrus* (Fig. 4A-C). Consistently with our *in vitro* analyses, suppression of Rab11 modified dendritic morphology similar to cultured neurons of 3 or 7 DIV (Fig. 4D-E), showing an increase on dendritic branching (Fig. 4F). In addition, we also quantified the number of dendritic spines in each condition. We found a significant reduction in the number of spines in Rab11-suppressed neurons compared to the control condition (Fig. 4G-H). Notably, this observation was consistent with our *in vitro* results obtained in 21 DIV Rab11-suppressed neurons (Fig. S2A-H), as well as with previous reports [22].

The contribution of Rab11 to dendritic growth described in this work prompted us to explore whether the loss of function of Rab11 could affect dendritic physiology. Therefore, we wondered whether local suppression of Rab11 in the hippocampus of adult rats would affect the long-term potentiation response (LTP) in this area. Figure 5 shows the experimental LTP paradigm used in this work, including stimulating/ recording electrodes position in hippocampal slices and setting for EPSP amplitude

recording at baseline, before and after LTP stimulus (Fig. 5A-B). When LTP was induced, by applying a strong stimulation paradigm such as the high frequency stimulation (HFS) protocol, LTP was achieved in both the shSc and shRab11 groups (Fig. 5C). The two-way repeated measures (RM) ANOVA showed a significant effect of time [F (5, 30) = 17.81; p = 0.0001], without treatment effect [F (1, 6) = 0.88; p = 0.3826] and interaction [F (5, 30) = 0.4728; p = 0.7935]. The Holm-Sidak multiple comparison test showed significant differences in the% of EPSP before (between -40 and -20 min) and after (0, 20, 40 and 60 min, p <0.05) of HFS stimulation in both groups. No differences were observed between groups in the subsequent times of the HFS stimulation (p> 0.05; Fig. 5C). However, when we evaluated LTP-induction sensitivity, the one-way ANOVA of RM showed that the TF protocol used could not induce LTP in shRab11 animal brain sections at any frequency assayed (40–100 HZ) [F (1,094, 3,283) = 1,180; p = 0.3592] (Fig. 5D). Accordingly, when we compared the shSc and shRab11 groups using this protocol, we found a significant effect on time [F (5, 30) = 7.08; p = 0.0002], treatment (shRab11 vs. shSc) [F (1, 6) = 27.24; p = 0.0020] and interaction [F (5, 30) = 13.88; p = 0.0001]. The Holm-Sidak multiple comparison test showed a significant increase in % of EPSP in the control group (shSc, 96.4 ± 32.8%) compared to their baseline EPSP after 40 Hz TF, and compared to each point of time of the shRab11 group, and this significant increase persisted for up to 60 minutes (Fig. 5D). The same frequency stimulation in the shRab11 group could not induce increases in EPSP% (-11.4 ± 8.2%; p <0.05) (Fig. 5E).

Together, these results suggest that Rab11 suppression reduces the number of spines in the dendrites and also the sensitivity to induce LTP in the hippocampal dentate gyrus *in vivo.*

### *3.5 The loss of function of Rab11 reduced hippocampal-dependent memory acquisition in adult rats*

Currently, learning and memory processes are focus on different regions of the brain, including the hippocampus. This is an area highly specialized in storing new declarative and episodic memories [54, 55]. This notion is based on the fact that the loss of this area leads to irreversible amnesia, without the possibility of forming new memories; although pre-existing memories remain unaltered. Furthermore, the hippocampus is key in modulating sensorimotor processes [56, 57].

Collectively, our results show that REs Rab11 control sub-cellular destination of somatodendritic proteins and the morphology of dendritic tree in hippocampal neurons *in vitro*. Furthermore, Rab11-suppressed neurons showed a significant decrease in the number of dendritic spines, impacting on the sensitivity to induce LTP *in vivo*. Based on these findings, we hypothesize that Rab11 is able to link structural changes of dendrites with their physiology. Therefore, we proposed to analyze whether REs Rab11 also modulates memory formation. Accordingly, associative learning and memory have been studied through standard Contextual Fear Conditioning (sCFC), a useful paradigm for studying learning and memory in both developing and adult brains [39, 58-60]. Thus, we conducted freezing (fear conditioning) and locomotion (OF) tests in adult rats expressing shRab11, by stereotaxic injections of lentiviral particles in the hippocampus, and then we measured both fear response and motor activity (Fig. 6A). We found that Rab11-suppressed animals (7 days after stereotaxic injection) showed a decrease in freezing time 24 h after receiving an aversive stimulus (footshock) in a visual and odor cues (conditioned stimulus; CS) compared to controls (for shRab11 after shock; $p= 0.014$, ANOVA, Fig. 6B). In contrast, no differences were observed on freezing time

before shock between shSc and shRab11 animals (p=0.13, ANOVA; Fig. 6B). These results suggest the participation of dorsal hippocampus in memory acquisition.

We also measured the number of rearing episodes (vertical movements), another characteristic of the exploratory behavior of rodents. This behavior was used as a recognition variable, where rats stand on hind legs and explore the context. Accordingly, a significant increase in the number of rearing episodes in Rab11-suppressed animals was observed compared to control animals. This behavior was observed only in Rab11-suppressed animals, both before and after the footshock (shRab11 before shock, p= 0.019; shRab11 after shock, p=0.036, ANOVA; Fig. 6C).

The locomotor activity was also measured, using an open field (OF) test 7 days after stereotaxis; these results suggest a significant increase in the time spent in horizontal activity in of the open field (seconds) and total distance traveled (meters) in Rab11-suppressed animals, compared to controls (shRab11 animals, p=0.01, ANOVA; Fig. 6D-E, respectively). Finally, we measured the time spent by animals in the center area; although Rab11-suppressed animals tended to spend more time, no significant differences with control animals were detected (Fig. 6F). Together, these results suggest that the increase on the exploratory behavior observed in Rab11-suppressed animals could rely on habituation failures to the environment [61].

## 4. Discussion

In this study we show a novel and fundamental roles of REs Rab11 not only in remodeling the morphology of the dendritic tree *in vitro*, but also in the regulation of neuronal activity *in vivo*. Accordingly, we characterized the sub-cellular distribution of REs Rab11 during the development of hippocampal neurons in culture from 1 to 21 DIV. In this regard, we observed a slight enrichment of REs Rab11 in the neuritic tip as well as in the central region of growth cones of 1 DIV neurons. These results are consistent with previous studies showing that, during the growth cone formation REs are require for the extension of the plasma membrane and replacement of membrane proteins [18, 62]. Moreover, in neurons cultured for 7 and 14 DIV, REs Rab11 segregated to dendrites, being mainly enriched in the proximal region. Finally, when neurons complete maturation (by 21 DIV), REs Rab11 were relocated showing a uniform distribution throughout dendrites. Together, these results suggest a dynamic distribution required to achieve the spatial demands of the neuron; by instance, to allow a proper delivery of proteins needed for membrane expansion during neuronal development.

Rab11 is able to control both axonal growth and postsynaptic architecture. In this regard, its overexpression promotes axon elongation of cortical neurons of the mouse brain, mediated by the lemur kinase 1 (LMTK1) and Cdk5 [24]. Also, Rab11 plays a role on the trafficking of integrins to axons and growth cones of peripheral neurons and PC12 cells [25]. Moreover, recent reports showed that Rab11 is critical to control the synapse architecture; in fact, Rab11 suppression decreases the distribution of AMPA receptor at cell surface and PSD-95 clusters at synapses [22].

Branching and density of dendrites are key to satisfy the physiological requirements of the neuronal activity; both are critical to process inputs received by the dendritic tree

[58, 59]. In fact, dendritic anomalies in neurological disorders have been often associated with cognitive impairments [60]. In this regard, neurons of transgenic *Drosophila melanogaster* larvae expressing human amyloid-β (Aβ42) showed an enhancement in neurite outgrowth and arborization before neurodegenerative symptom [63]. In addition, Soltani et al. [64] analyzed the effect of Engrailed (En1 and En2 proteins encoded by an autism susceptibility gene) in dendritogenesis or synaptogenesis; both En1 and En2 over-expression increased the complexity of the dendritic tree. However, En1 increased the density of dendritic spines; although En2 had less effect on spines density. In Down syndrome infants (younger than 6 months old), dendritic branching and length was enhanced compared to controls. These measures were reversed in subjects older than 2 years, and these dendritic parameters were lower than in controls [65]. Our results show that reducing Rab11 expression in neurons leads to an increase of primary neurites at early stages (3 DIV) paralleled by an increase of dendritic branching; nevertheless, total length of dendrites remained unaltered. Furthermore, we also observed a reduction in the number of dendritic spines, reproducing the phenotype reported in Esteves da Silva et al [22].

Considering these results, we hypothesize that, in hippocampal neurons, a well-balanced expression and distribution of REs Rab11 is instrumental for a proper dendritic tree arborization during development, in addition to its previously characterized role on spines formation.

It is widely accepted that a segregated flow of proteins to axons and dendrites is critical to maintain their identities, highlighting the relevance of the endosomal trafficking able to regulate the differentiation of neuronal domains [15, 21, 24, 66, 67]. The alterations that we reported in Rab11-suppressed neurons also affect hippocampal protein dynamics of cultured neurons and, consequently, their proper development.

Specifically, the proper localization of TfR and mGluR1, was disrupted under Rab11 suppression, since they were incorrectly located in the axonal compartment. These data support the idea that Rab11 suppression produces dendritic abnormalities, not only in the dendritic tree morphology but also in dendritic protein localization. In this regard, changes in the morphology of dendritic spines could be altered by manipulations affecting intracellular calcium and correlated with alterations in synaptic plasticity [68, 69]. Selective stimulation of mGluR1 increased the length of dendritic spines of dendrites in both organotypic and isolated cell culture of hippocampal neurons [70]. *In vivo* studies have shown the involvement of mGluR1 in spatial and associative learning, whereas *in vitro* studies described its participation in cLTP (chemical LTP) [71-73].

Moreover, we show that the functionality of hippocampal neurons is affected once Rab11is suppressed *in vivo*. We based this affirmation on the following evidence. We found an increased dendritic branching and decreased spines number both *in vitro* and *in vivo* after Rab11-suppression. These dendritic alterations have a significant impact on hippocampal synaptic transmission (that could be extended to dentate gyrus because the infection was also evident in this area). When adult rats were infected with shRab11 within the CA1, the sensitivity to induce LTP in the dentate gyrus was reduced, since they were unable to induce LTP (using TF protocol up to 100 Hz). In contrast, in control animals LTP was achieved at 40 Hz. It is important to highlight that Rab11 suppression did not completely abolish the capacity to generate LTP because the HFS protocol was able to induce LTP in both shRab11 and shSc groups. Dentate gyrus, a hippocampal subregion, is the first synaptic contact of input information arising the hippocampus from the entorrinal cortex, through the perforant pathway [74, 75] which in turn connects to the CA3–CA1 circuitry forming the intrahippocampal ‘‘trisynaptic loop’’[76]. It has been shown that activity of the dentate gyrus can by modified by the

synchronous population events of both the entorhinal input (feed-forward path) and the CA3-CA1 recurrent system (feed-back path) [77]. Also, infusion of different modulators into the CA1 modifies dentate gyrus synaptic plasticity [78-80]. Our results may indicate that the whole hippocampal three-synaptic loop was affected by Rab11 suppression in CA1, making the post-synapses in the dentate gyrus less sensitive to priming stimulation of the perforant pathway.

The hippocampal LTP was identified as a potential neural substrate for the acquisition and storage of hippocampal-dependent memories [81-85]. Interestingly, we observed changes in the behavior of those animals infected with shRab11, showing a reduced performance in spatial memory-related behaviors and hyperactivity compared to animals under physiological conditions. The combination of odor and visual cues used in contextual fear conditioning test strengthen the participation of hippocampus in contextual memory. Although we suggest that the hippocampus may be involved in contextual learning under these circumstances, we cannot discard the participation of other brain areas [86-88]. We also observed that Rab11-suppressed animals increase locomotor activity, suggesting that these animals have some degree of hyperactivity or motor circuit alterations. In this regard, there is evidence arguing that the increased in locomotion after lesions of the dorsal hippocampus may result from damage of the fibers that extend from the subiculum to the nucleus accumbens (nucleus that regulate the exploration necessary for the acquisition of information about the features of the context) and then additional hippocampal areas would receive poor information [89, 90]. Although a close relationship has been described between Rabs and cognitive functions [19], there are exceptions. In mice Rab3A mutants, hippocampal CA3 mossy fibers LTD and LTP were removed, however the hippocampal-dependent learning test was normal [91].

The contribution of the endocytic machinery in the polarization of neuronal cell domains has been well characterized [47, 92]. Accordingly, our results propose that changes in the expression of REs Rab11 during neuronal development affect both the maturation of the somatodendritic domain of hippocampal neurons *in vitro* and the maintenance of synaptic transmission, as well as memory formation and behavior in adult animals (Fig. 7).

Finally, several studies link the participation of Rab11 in neurodegenerative disorders, such as Alzheimer's, Huntington's and Parkinson's diseases [93-97], in which the loss of neurons and the reduction of synapses correlates with cognitive deficits. Our findings contribute to unveil the physiological relevance of REs Rab11 in higher organisms, as well as their associated *in vivo* functions. Therefore, REs Rab11 are crucial not only for the correct development of neuronal compartments, but also to allow functional maturation of neurons, neural activity and acquisition of spatial memory.

**Acknowledgements:**

Research at the Laboratory of Neurobiology at INIMEC-CONICET-UNC is supported by grants from the National Agency for Scientific and Technological Promotion of Argentina, FONCyT (PICT 2014-2119). MFP and CC are staff scientists of the National Council of Research of Argentina (CONICET). SOS and EAV are doctoral fellows (CONICET). VRS and MSG are postdoctoral fellows (CONICET). The authors greatly acknowledge the Centro de Micro y Nanoscopía de Córdoba (CEMINCO) for technical and imaging assistance, Carlos Wilson for critical reading of the manuscript and Joss Heywood for the English edition of the manuscript.

**Competing interests:** No competing interests declared.

## References


1. Zerial, M. & McBride, H. (2001) Rab proteins as membrane organizers, *Nat Rev Mol Cell Biol.* **2**, 107-17.
2. Stenmark, H. (2009) Rab GTPases as coordinators of vesicle traffic, *Nat Rev Mol Cell Biol.* **10**, 513-25.
3. Wandinger-Ness, A. & Zerial, M. (2014) Rab proteins and the compartmentalization of the endosomal system, *Cold Spring Harb Perspect Biol.* **6**, a022616.
4. Lock, J. G. & Stow, J. L. (2005) Rab11 in recycling endosomes regulates the sorting and basolateral transport of E-cadherin, *Mol Biol Cell.* **16**, 1744-55.
5. Mrozowska, P. S. & Fukuda, M. (2016) Regulation of podocalyxin trafficking by Rab small GTPases in epithelial cells, *Small GTPases.* **7**, 231-238.
6. Urbe, S., Huber, L. A., Zerial, M., Tooze, S. A. & Parton, R. G. (1993) Rab11, a small GTPase associated with both constitutive and regulated secretory pathways in PC12 cells, *FEBS Lett.* **334**, 175-82.
7. Casanova, J. E., Wang, X., Kumar, R., Bhartur, S. G., Navarre, J., Woodrum, J. E., Altschuler, Y., Ray, G. S. & Goldenring, J. R. (1999) Association of Rab25 and Rab11a with the apical recycling system of polarized Madin-Darby canine kidney cells, *Mol Biol Cell.* **10**, 47-61.
8. van der Wouden, J. M., Maier, O., van, I. S. C. & Hoekstra, D. (2003) Membrane dynamics and the regulation of epithelial cell polarity, *Int Rev Cytol.* **226**, 127-64.
9. Powelka, A. M., Sun, J., Li, J., Gao, M., Shaw, L. M., Sonnenberg, A. & Hsu, V. W. (2004) Stimulation-dependent recycling of integrin beta1 regulated by ARF6 and Rab11, *Traffic.* **5**, 20-36.
10. Ullrich, O., Reinsch, S., Urbe, S., Zerial, M. & Parton, R. G. (1996) Rab11 regulates recycling through the pericentriolar recycling endosome, *The Journal of cell biology.* **135**, 913-24.
11. Maxfield, F. R. & McGraw, T. E. (2004) Endocytic recycling, *Nat Rev Mol Cell Biol.* **5**, 121-32.
12. Goldenring, J. R. (2015) Recycling endosomes, *Curr Opin Cell Biol.* **35**, 117-22.
13. Conde, C. & Caceres, A. (2009) Microtubule assembly, organization and dynamics in axons and dendrites, *Nat Rev Neurosci.* **10**, 319-32.
14. van Beuningen, S. F. & Hoogenraad, C. C. (2016) Neuronal polarity: remodeling microtubule organization, *Current opinion in neurobiology.* **39**, 1-7.
15. Horton, A. C. & Ehlers, M. D. (2003) Neuronal polarity and trafficking, *Neuron.* **40**, 277-95.
16. Horton, A. C., Racz, B., Monson, E. E., Lin, A. L., Weinberg, R. J. & Ehlers, M. D. (2005) Polarized secretory trafficking directs cargo for asymmetric dendrite growth and morphogenesis, *Neuron.* **48**, 757-71.
17. Bisbal, M., Conde, C., Donoso, M., Bollati, F., Sesma, J., Quiroga, S., Diaz Anel, A., Malhotra, V., Marzolo, M. P. & Caceres, A. (2008) Protein kinase d regulates trafficking of dendritic membrane proteins in developing neurons, *The Journal of neuroscience : the official journal of the Society for Neuroscience.* **28**, 9297-308.
18. Li, X. & DiFiglia, M. (2012) The recycling endosome and its role in neurological disorders, *Prog Neurobiol.* **97**, 127-41.
19. D'Adamo, P., Masetti, M., Bianchi, V., More, L., Mignogna, M. L., Giannandrea, M. & Gatti, S. (2014) RAB GTPases and RAB-interacting proteins and their role in the control of cognitive functions, *Neurosci Biobehav Rev.* **46 Pt 2**, 302-14.
20. Sann, S., Wang, Z., Brown, H. & Jin, Y. (2009) Roles of endosomal trafficking in neurite outgrowth and guidance, *Trends Cell Biol.* **19**, 317-24.
21. Park, M., Penick, E. C., Edwards, J. G., Kauer, J. A. & Ehlers, M. D. (2004) Recycling endosomes supply AMPA receptors for LTP, *Science.* **305**, 1972-5.

22. Esteves da Silva, M., Adrian, M., Schatzle, P., Lipka, J., Watanabe, T., Cho, S., Futai, K., Wierenga, C. J., Kapitein, L. C. & Hoogenraad, C. C. (2015) Positioning of AMPA Receptor-Containing Endosomes Regulates Synapse Architecture, *Cell Rep.* **13**, 933-43.
23. Ascano, M., Richmond, A., Borden, P. & Kuruvilla, R. (2009) Axonal targeting of Trk receptors via transcytosis regulates sensitivity to neurotrophin responses, *The Journal of neuroscience : the official journal of the Society for Neuroscience.* **29**, 11674-85.
24. Takano, T., Tomomura, M., Yoshioka, N., Tsutsumi, K., Terasawa, Y., Saito, T., Kawano, H., Kamiguchi, H., Fukuda, M. & Hisanaga, S. (2012) LMTK1/AATYK1 is a novel regulator of axonal outgrowth that acts via Rab11 in a Cdk5-dependent manner, *The Journal of neuroscience : the official journal of the Society for Neuroscience.* **32**, 6587-99.
25. Eva, R., Dassie, E., Caswell, P. T., Dick, G., ffrench-Constant, C., Norman, J. C. & Fawcett, J. W. (2010) Rab11 and its effector Rab coupling protein contribute to the trafficking of beta 1 integrins during axon growth in adult dorsal root ganglion neurons and PC12 cells, *The Journal of neuroscience : the official journal of the Society for Neuroscience.* **30**, 11654-69.
26. Lazo, O. M., Gonzalez, A., Ascano, M., Kuruvilla, R., Couve, A. & Bronfman, F. C. (2013) BDNF regulates Rab11-mediated recycling endosome dynamics to induce dendritic branching, *The Journal of neuroscience : the official journal of the Society for Neuroscience.* **33**, 6112-22.
27. Koseki, H., Donega, M., Lam, B. Y., Petrova, V., van Erp, S., Yeo, G. S., Kwok, J. C., Ffrench-Constant, C., Eva, R. & Fawcett, J. W. (2017) Selective rab11 transport and the intrinsic regenerative ability of CNS axons, *Elife.* **6**.
28. Nishino, H., Saito, T., Wei, R., Takano, T., Tsutsumi, K., Taniguchi, M., Ando, K., Tomomura, M., Fukuda, M. & Hisanaga, S. I. (2019) The LMTK1-TBC1D9B-Rab11A Cascade Regulates Dendritic Spine Formation via Endosome Trafficking, *The Journal of neuroscience : the official journal of the Society for Neuroscience.* **39**, 9491-9502.
29. Kawauchi, T., Sekine, K., Shikanai, M., Chihama, K., Tomita, K., Kubo, K., Nakajima, K., Nabeshima, Y. & Hoshino, M. (2010) Rab GTPases-dependent endocytic pathways regulate neuronal migration and maturation through N-cadherin trafficking, *Neuron.* **67**, 588-602.
30. Kaech, S. & Banker, G. (2006) Culturing hippocampal neurons, *Nat Protoc.* **1**, 2406-15.
31. Rubinson, D. A., Dillon, C. P., Kwiatkowski, A. V., Sievers, C., Yang, L., Kopinja, J., Rooney, D. L., Zhang, M., Ihrig, M. M., McManus, M. T., Gertler, F. B., Scott, M. L. & Van Parijs, L. (2003) A lentivirus-based system to functionally silence genes in primary mammalian cells, stem cells and transgenic mice by RNA interference, *Nat Genet.* **33**, 401-6.
32. Schindelin, J., Arganda-Carreras, I., Frise, E., Kaynig, V., Longair, M., Pietzsch, T., Preibisch, S., Rueden, C., Saalfeld, S., Schmid, B., Tinevez, J. Y., White, D. J., Hartenstein, V., Eliceiri, K., Tomancak, P. & Cardona, A. (2012) Fiji: an open-source platform for biological-image analysis, *Nat Methods.* **9**, 676-82.
33. Ferreira, T. A., Blackman, A. V., Oyrer, J., Jayabal, S., Chung, A. J., Watt, A. J., Sjostrom, P. J. & van Meyel, D. J. (2014) Neuronal morphometry directly from bitmap images, *Nat Methods.* **11**, 982-4.
34. Sholl, D. A. (1953) Dendritic organization in the neurons of the visual and motor cortices of the cat, *J Anat.* **87**, 387-406.
35. Chapleau, C. A. & Pozzo-Miller, L. (2012) Divergent roles of p75NTR and Trk receptors in BDNF's effects on dendritic spine density and morphology, *Neural Plast.* **2012**, 578057.
36. Conde, C., Arias, C., Robin, M., Li, A., Saito, M., Chuang, J. Z., Nairn, A. C., Sung, C. H. & Caceres, A. (2010) Evidence for the involvement of Lfc and Tctex-1 in axon formation, *The Journal of neuroscience : the official journal of the Society for Neuroscience.* **30**, 6793-800.
37. Teyler, T. J. & DiScenna, P. (1987) Long-term potentiation, *Annu Rev Neurosci.* **10**, 131-61.
38. Perez, M. F., Gabach, L. A., Almiron, R. S., Carlini, V. P., De Barioglio, S. R. & Ramirez, O. A. (2010) Different chronic cocaine administration protocols induce changes on dentate gyrus plasticity and hippocampal dependent behavior, *Synapse.* **64**, 742-53.

39. Sanders, M. J., Wiltgen, B. J. & Fanselow, M. S. (2003) The place of the hippocampus in fear conditioning, *European journal of pharmacology.* **463**, 217-23.
40. Xu, X. H., Deng, C. Y., Liu, Y., He, M., Peng, J., Wang, T., Yuan, L., Zheng, Z. S., Blackshear, P. J. & Luo, Z. G. (2014) MARCKS regulates membrane targeting of Rab10 vesicles to promote axon development, *Cell Res.* **24**, 576-94.
41. Zou, W., Yadav, S., DeVault, L., Nung Jan, Y. & Sherwood, D. R. (2015) RAB-10-Dependent Membrane Transport Is Required for Dendrite Arborization, *PLoS Genet.* **11**, e1005484.
42. Falk, J., Konopacki, F. A., Zivraj, K. H. & Holt, C. E. (2014) Rab5 and Rab4 regulate axon elongation in the Xenopus visual system, *The Journal of neuroscience : the official journal of the Society for Neuroscience.* **34**, 373-91.
43. Tang, B. L. (2001) Protein trafficking mechanisms associated with neurite outgrowth and polarized sorting in neurons, *J Neurochem.* **79**, 923-30.
44. Saxena, S., Bucci, C., Weis, J. & Kruttgen, A. (2005) The small GTPase Rab7 controls the endosomal trafficking and neuritogenic signaling of the nerve growth factor receptor TrkA, *The Journal of neuroscience : the official journal of the Society for Neuroscience.* **25**, 10930-40.
45. Lasiecka, Z. M., Yap, C. C., Caplan, S. & Winckler, B. (2010) Neuronal early endosomes require EHD1 for L1/NgCAM trafficking, *The Journal of neuroscience : the official journal of the Society for Neuroscience.* **30**, 16485-97.
46. Wang, T., Liu, Y., Xu, X. H., Deng, C. Y., Wu, K. Y., Zhu, J., Fu, X. Q., He, M. & Luo, Z. G. (2011) Lgl1 activation of rab10 promotes axonal membrane trafficking underlying neuronal polarization, *Dev Cell.* **21**, 431-44.
47. Taylor, C. A., Yan, J., Howell, A. S., Dong, X. & Shen, K. (2015) RAB-10 Regulates Dendritic Branching by Balancing Dendritic Transport, *PLoS Genet.* **11**, e1005695.
48. Ren, M., Xu, G., Zeng, J., De Lemos-Chiarandini, C., Adesnik, M. & Sabatini, D. D. (1998) Hydrolysis of GTP on rab11 is required for the direct delivery of transferrin from the pericentriolar recycling compartment to the cell surface but not from sorting endosomes, *Proceedings of the National Academy of Sciences of the United States of America.* **95**, 6187-92.
49. Pandey, S., Mahato, P. K. & Bhattacharyya, S. (2014) Metabotropic glutamate receptor 1 recycles to the cell surface in protein phosphatase 2A-dependent manner in non-neuronal and neuronal cell lines, *Journal of neurochemistry.* **131**, 602-14.
50. Burack, M. A., Silverman, M. A. & Banker, G. (2000) The role of selective transport in neuronal protein sorting, *Neuron.* **26**, 465-72.
51. Sampo, B., Kaech, S., Kunz, S. & Banker, G. (2003) Two distinct mechanisms target membrane proteins to the axonal surface, *Neuron.* **37**, 611-24.
52. Cheng, P. L., Song, A. H., Wong, Y. H., Wang, S., Zhang, X. & Poo, M. M. (2011) Self-amplifying autocrine actions of BDNF in axon development, *Proceedings of the National Academy of Sciences of the United States of America.* **108**, 18430-5.
53. Cheng, P. L. & Poo, M. M. (2012) Early events in axon/dendrite polarization, *Annu Rev Neurosci.* **35**, 181-201.
54. Vanderwolf, C. H. & Cain, D. P. (1994) The behavioral neurobiology of learning and memory: a conceptual reorientation, *Brain Res Brain Res Rev.* **19**, 264-97.
55. Cahill, L., McGaugh, J. L. & Weinberger, N. M. (2001) The neurobiology of learning and memory: some reminders to remember, *Trends Neurosci.* **24**, 578-81.
56. Bast, T. & Feldon, J. (2003) Hippocampal modulation of sensorimotor processes, *Prog Neurobiol.* **70**, 319-45.
57. van Lier, H., Coenen, A. M. & Drinkenburg, W. H. (2003) Behavioral transitions modulate hippocampal electroencephalogram correlates of open field behavior in the rat: support for a sensorimotor function of hippocampal rhythmical synchronous activity, *The Journal of neuroscience : the official journal of the Society for Neuroscience.* **23**, 2459-65.

58. Losonczy, A., Makara, J. K. & Magee, J. C. (2008) Compartmentalized dendritic plasticity and input feature storage in neurons, *Nature.* **452**, 436-41.
59. Spruston, N. (2008) Pyramidal neurons: dendritic structure and synaptic integration, *Nat Rev Neurosci.* **9**, 206-21.
60. Kaufmann, W. E. & Moser, H. W. (2000) Dendritic anomalies in disorders associated with mental retardation, *Cereb Cortex.* **10**, 981-91.
61. Fanselow, M. S. (2000) Contextual fear, gestalt memories, and the hippocampus, *Behav Brain Res.* **110**, 73-81.
62. Yap, C. C. & Winckler, B. (2012) Harnessing the power of the endosome to regulate neural development, *Neuron.* **74**, 440-51.
63. Saad, Y., Segal, D. & Ayali, A. (2015) Enhanced neurite outgrowth and branching precede increased amyloid-beta-induced neuronal apoptosis in a novel Alzheimer's disease model, *J Alzheimers Dis.* **43**, 993-1006.
64. Soltani, A., Lebrun, S., Carpentier, G., Zunino, G., Chantepie, S., Maiza, A., Bozzi, Y., Desnos, C., Darchen, F. & Stettler, O. (2017) Increased signaling by the autism-related Engrailed-2 protein enhances dendritic branching and spine density, alters synaptic structural matching, and exaggerates protein synthesis, *PLoS One.* **12**, e0181350.
65. Becker, L. E., Armstrong, D. L. & Chan, F. (1986) Dendritic atrophy in children with Down's syndrome, *Ann Neurol.* **20**, 520-6.
66. Park, M., Salgado, J. M., Ostroff, L., Helton, T. D., Robinson, C. G., Harris, K. M. & Ehlers, M. D. (2006) Plasticity-induced growth of dendritic spines by exocytic trafficking from recycling endosomes, *Neuron.* **52**, 817-30.
67. Arias, C. I., Siri, S. O. & Conde, C. (2015) Involvement of SARA in Axon and Dendrite Growth, *PLoS One.* **10**, e0138792.
68. Kasai, H., Fukuda, M., Watanabe, S., Hayashi-Takagi, A. & Noguchi, J. (2010) Structural dynamics of dendritic spines in memory and cognition, *Trends in neurosciences.* **33**, 121-9.
69. Niswender, C. M. & Conn, P. J. (2010) Metabotropic glutamate receptors: physiology, pharmacology, and disease, *Annual review of pharmacology and toxicology.* **50**, 295-322.
70. Vanderklish, P. W. & Edelman, G. M. (2002) Dendritic spines elongate after stimulation of group 1 metabotropic glutamate receptors in cultured hippocampal neurons, *Proceedings of the National Academy of Sciences of the United States of America.* **99**, 1639-44.
71. Neyman, S. & Manahan-Vaughan, D. (2008) Metabotropic glutamate receptor 1 (mGluR1) and 5 (mGluR5) regulate late phases of LTP and LTD in the hippocampal CA1 region in vitro, *The European journal of neuroscience.* **27**, 1345-52.
72. Aiba, A., Chen, C., Herrup, K., Rosenmund, C., Stevens, C. F. & Tonegawa, S. (1994) Reduced hippocampal long-term potentiation and context-specific deficit in associative learning in mGluR1 mutant mice, *Cell.* **79**, 365-75.
73. Mannaioni, G., Marino, M. J., Valenti, O., Traynelis, S. F. & Conn, P. J. (2001) Metabotropic glutamate receptors 1 and 5 differentially regulate CA1 pyramidal cell function, *J Neurosci.* **21**, 5925-34.
74. Leranth, C. & Hajszan, T. (2007) Extrinsic afferent systems to the dentate gyrus, *Progress in brain research.* **163**, 63-84.
75. Goodrich-Hunsaker, N. J., Hunsaker, M. R. & Kesner, R. P. (2008) The interactions and dissociations of the dorsal hippocampus subregions: how the dentate gyrus, CA3, and CA1 process spatial information, *Behavioral neuroscience.* **122**, 16-26.
76. Amaral, D. G. & Witter, M. P. (1989) The three-dimensional organization of the hippocampal formation: a review of anatomical data, *Neuroscience.* **31**, 571-91.
77. Penttonen, M., Kamondi, A., Sik, A., Acsady, L. & Buzsaki, G. (1997) Feed-forward and feed-back activation of the dentate gyrus in vivo during dentate spikes and sharp wave bursts, *Hippocampus.* **7**, 437-50.

78. Glaser, V., Carlini, V. P., Gabach, L., Ghersi, M., de Barioglio, S. R., Ramirez, O. A., Perez, M. F. & Latini, A. (2010) The intra-hippocampal leucine administration impairs memory consolidation and LTP generation in rats, *Cellular and molecular neurobiology.* **30**, 1067-75.
79. Carlini, V. P., Ghersi, M., Gabach, L., Schioth, H. B., Perez, M. F., Ramirez, O. A., Fiol de Cuneo, M. & de Barioglio, S. R. (2011) Hippocampal effects of neuronostatin on memory, anxiety-like behavior and food intake in rats, *Neuroscience.* **197**, 145-52.
80. Ghersi, M. S., Gabach, L. A., Buteler, F., Vilcaes, A. A., Schioth, H. B., Perez, M. F. & de Barioglio, S. R. (2015) Ghrelin increases memory consolidation through hippocampal mechanisms dependent on glutamate release and NR2B-subunits of the NMDA receptor, *Psychopharmacology.* **232**, 1843-57.
81. Bliss, T. V. & Lomo, T. (1973) Long-lasting potentiation of synaptic transmission in the dentate area of the anaesthetized rabbit following stimulation of the perforant path, *J Physiol.* **232**, 331-56.
82. Phillips, R. G. & LeDoux, J. E. (1992) Differential contribution of amygdala and hippocampus to cued and contextual fear conditioning, *Behav Neurosci.* **106**, 274-85.
83. Bliss, T. V. & Collingridge, G. L. (1993) A synaptic model of memory: long-term potentiation in the hippocampus, *Nature.* **361**, 31-9.
84. Martin, S. J., Grimwood, P. D. & Morris, R. G. (2000) Synaptic plasticity and memory: an evaluation of the hypothesis, *Annu Rev Neurosci.* **23**, 649-711.
85. Izquierdo, I., Cammarota, M., Da Silva, W. C., Bevilaqua, L. R., Rossato, J. I., Bonini, J. S., Mello, P., Benetti, F., Costa, J. C. & Medina, J. H. (2008) The evidence for hippocampal long-term potentiation as a basis of memory for simple tasks, *An Acad Bras Cienc.* **80**, 115-27.
86. Levy, D. A., Hopkins, R. O. & Squire, L. R. (2004) Impaired odor recognition memory in patients with hippocampal lesions, *Learn Mem.* **11**, 794-6.
87. Wiltgen, B. J., Sanders, M. J., Anagnostaras, S. G., Sage, J. R. & Fanselow, M. S. (2006) Context fear learning in the absence of the hippocampus, *The Journal of neuroscience : the official journal of the Society for Neuroscience.* **26**, 5484-91.
88. Conejo, N. M., Gonzalez-Pardo, H., Lopez, M., Cantora, R. & Arias, J. L. (2007) Induction of c-Fos expression in the mammillary bodies, anterior thalamus and dorsal hippocampus after fear conditioning, *Brain Res Bull.* **74**, 172-7.
89. Westbrook, R. F., Good, A. J. & Kiernan, M. J. (1997) Microinjection of morphine into the nucleus accumbens impairs contextual learning in rats, *Behav Neurosci.* **111**, 996-1013.
90. Legault, M. & Wise, R. A. (1999) Injections of N-methyl-D-aspartate into the ventral hippocampus increase extracellular dopamine in the ventral tegmental area and nucleus accumbens, *Synapse.* **31**, 241-9.
91. Castillo, P. E., Janz, R., Sudhof, T. C., Tzounopoulos, T., Malenka, R. C. & Nicoll, R. A. (1997) Rab3A is essential for mossy fibre long-term potentiation in the hippocampus, *Nature.* **388**, 590-3.
92. Takano, T., Urushibara, T., Yoshioka, N., Saito, T., Fukuda, M., Tomomura, M. & Hisanaga, S. (2014) LMTK1 regulates dendritic formation by regulating movement of Rab11A-positive endosomes, *Mol Biol Cell.* **25**, 1755-68.
93. DiFiglia, M., Sapp, E., Chase, K., Schwarz, C., Meloni, A., Young, C., Martin, E., Vonsattel, J. P., Carraway, R., Reeves, S. A. & et al. (1995) Huntingtin is a cytoplasmic protein associated with vesicles in human and rat brain neurons, *Neuron.* **14**, 1075-81.
94. Richards, P., Didszun, C., Campesan, S., Simpson, A., Horley, B., Young, K. W., Glynn, P., Cain, K., Kyriacou, C. P., Giorgini, F. & Nicotera, P. (2011) Dendritic spine loss and neurodegeneration is rescued by Rab11 in models of Huntington's disease, *Cell Death Differ.* **18**, 191-200.

95. Li, X., Sapp, E., Valencia, A., Kegel, K. B., Qin, Z. H., Alexander, J., Masso, N., Reeves, P., Ritch, J. J., Zeitlin, S., Aronin, N. & Difiglia, M. (2008) A function of huntingtin in guanine nucleotide exchange on Rab11, *Neuroreport.* **19**, 1643-7.
96. Udayar, V., Buggia-Prevot, V., Guerreiro, R. L., Siegel, G., Rambabu, N., Soohoo, A. L., Ponnusamy, M., Siegenthaler, B., Bali, J., Simons, M., Ries, J., Puthenveedu, M. A., Hardy, J., Thinakaran, G. & Rajendran, L. (2013) A paired RNAi and RabGAP overexpression screen identifies Rab11 as a regulator of beta-amyloid production, *Cell Rep.* **5**, 1536-51.
97. Breda, C., Nugent, M. L., Estranero, J. G., Kyriacou, C. P., Outeiro, T. F., Steinert, J. R. & Giorgini, F. (2015) Rab11 modulates alpha-synuclein-mediated defects in synaptic transmission and behaviour, *Hum Mol Genet.* **24**, 1077-91.

**Figure legends**

**Figure 1. Sub-cellular distribution of Rab11 recycling endosomes in hippocampal neurons during development.** (**A-J**) Representative images of hippocampal neurons immunostained with anti-Rab11 (green; **A', C', E', G', I'**) or plus anti-Tyr Tubulin (red; **A, C. E, G, I**) at 1, 3, 7 and 21 DIV. Pseudocolor (Fire-LUT) view (**B, D, F, H, J**) of the boxes in images **A, C, E, G,** and **I**. Arrows point to Rab11 while the arrowheads indicate regions without Rab11 endosomes. Magnifications show the presence of REs Rab11 in the process at each experimental time. (**K**) The number of proximal Rab11-positive puncta (10 μm from soma) at 1, 3, 7, 14 and 21 DIV was quantified. (**L**) Quantification of the number of Rab11-positive puncta (10 μm from neurite tip) at 3 and 7DIV. The data are presented as the mean ± SEM; ***p <0.001; ****p <0.0001 One-way ANOVA and Tukey's multiple comparisons test; n=53 (**K**) and n=76 (**L**) from 3 independent experiments. Scale bar: 20μm. Fire-LUT scale bar: 10μm.

**Figure 2. Suppression of Rab11 produces changes in both the number and length of the dendritic branching of hippocampal neurons.** (**A-B**) Hippocampal neurons were electroporated with shSc, shRab11 and observed with confocal microscopy at 3 DIV (**A**) and 7 DIV (**B**). Acquired Z-stacks were integrated and inverted for morphometric analysis. Higher-magnification views of the somatodendritic domain.

Scale Bar: 10 μm (box bottom). (**C, E**) Scatter plot obtained from Sholl analysis of the number of interactions from soma until 300 μm to MAP2+ neurites in the somatodendritic domain at 3 DIV (**C**) and 7 DIV (**E**). (**D, F**) Quantification of branching order for 3 DIV (**D**) and 7 DIV (**F**) hippocampal neurons. The data are presented as the mean ± SEM. *p> 0.05** p <0.01*** p <0.001, Student's t-test, n=31 for each condition. (**G**) Quantification of the number of primary processes. (**H**) Quantification of total neurite length in Rab11-suppressed neurons at 3 and 7 DIV. The data are presented as the mean ± SEM. *p> 0.05** p <0.01*** p <0.001, Student's t-test, n=29 for each condition from 3 independent experiments.

**Figure 3. Suppression of Rab11 alters the intracellular distribution of somatodendritic proteins**. Confocal images of hippocampal neurons (3 DIV) transfected with shSc or shRab11 and immunostained with anti-transferrin receptor (TfR) (red) and anti-MAP2 (blue) (**A-B**); anti-c-Myc (red) and anti-Tau (blue) (**C-D**); and anti-VAMP2 (red) and anti-MAP2 (blue) (**E-F**). The arrows point to the axons. Scale bar: 20μm. (**G-H**) Quantification of polarity index of somatodendritic receptors in neurons shSc and Rab11 suppressed at 3 DIV (**G**) and 7 DIV (**H**). The data are presented as the mean ± SEM. p> 0.05* p <0.01, Student's t-test. mGluR1, n=39 and n=34; TfR, n=33 and n=40; VAMP2, n=26 and n=24, for shSc and shRab11 respectively, from 3 independent experiments.

**Figure 4**. ***In vivo*** **suppression of Rab11 produces changes in the number of the spines and dendritic complexity.** (**A-C**) Representative images of histological section of the rat brain after stereotaxic showing the location site of the cannula immunostained with DAPI to show the nuclei (blue) (**B**) and the infection efficiency of the viral particles in the hippocampus (green) (**C**). (**D**) Representative images of infected neurons

(with shSc or shRab11) and the magnification to show the dendritic tree in each experimental condition. Neurons Rab11-suppressed present a more complex dendritic tree (red arrows) compared to control neurons (white arrows). (**E**) Representative images of the 3D reconstruction of the dendritic complexity of Rab11- suppressed and control neurons, and the quantification of the branching points for each condition (**F**). (**G**) Representative images of dendritic spines of neurons infected with shSc-GFP or shRab11-GFP, and the quantification of the spines number for each condition (**H**). The data are presented as the mean ± SEM. *** p <0.001, Student's t-test, n=20 for each condition from at least 3 animals.

**Figure 5**. ***In vivo*** **suppression of Rab11 reduced sensitivity to induce LTP in hippocampal neurons.** (**A**) Hippocampal slice cartoon indicating the position of stimulation and recording electrodes. (**B**) Field excitatory postsynaptic potential (EPSP) sample traces showing how EPSP were measured. (**C**) Time course graph showing increments in EPSP amplitude expressed as % of basal EPSP after high-frequency stimulation protocol (HFS), in shSc (n=4) and shRab11 (n=4) groups, *p < 0.05 compared to basal (-40 and -20 min) in both groups. (**D**) Time course graph showing increments in EPSP amplitude expressed as % of basal EPSP after threshold frequency (TF) protocol, in shSc (n=4) and shRab11 (n=4) groups, *p < 0.05 compared to basal (-40 and -20 min) and to all time points from the shRab11 group. In C and D graphs the values represent mean ± SEM. (**E**) Input-output curve for shRab11 group, showing that the EPSP amplitude after each stimulation frequency was comparable to basal, indicating that LTP was not induced at any frequency tested (n=4). Scale bar: 10µm.

**Figure 6**. **Hippocampal suppression of Rab11 reduced hippocampal-dependent memory acquisition in adult rats**. (**A**) Schematic image of the experimental design for

behavior analysis of the animals infected with lentivirus carrying shSc or shRab11. The animals are placed in conditional chambers 6 days after infection. Quantification of freezing (%) (**B**), Number of rearing (**C**), indicating the values pre (before) and post-shock (after). Time spent in horizontal activity (sec) (**D**), Total distance traveled (m) (**E**) and Time in the center area (%) (**F**) were measured. Time spent in horizontal activity is the time used by the animal horizontal movements or locomotion on the OF to each recording time. The data are presented as the mean ± SEM. * $p < 0.05$, Student's t-test, n=10 animals for each condition.

**Figure 7**. **Rab11 endosomes regulate neuronal activity, behavior, and memory in adult rats**. Schematic representation highlighting how REs Rab11 modulate dendritic morphology and become a key event to regulate neuronal activity and higher brain functions, such as memory and behavior.

**Supplementary Figure 1: Measurement of the shRab11efficiency.** (**A**) Western blots images representative of neurons transfected with shSc or shRab11-1 and shRab11-2 and revealed against anti-Rab11 and anti-tubulin. (**B**) Quantification of the suppression efficiency of shRab11. The data are presented as the mean ± SEM; ***p: 0.001; One-way ANOVA and Tukey´s multiple comparisons test from 3 independent experiments.

**Supplementary Figure 2: The suppression of Rab11 decreases the number of dendritic spines in mature neurons.** (**A-H**) Representative images of dendritic spines of neurons electroporated with shSc-GFP (**A-D**) or with shRab11-GFP (**E-H**) and immunostained for PSD95 (red). Arrows show dendritic spines positive for PSD95 (**B-D, F-H**) while asterisks show dendritic spines negative for PSD95 (**F-H**). Scale bar: 5µm.

**CRediT Author Statement**

Author contributions

- **Sebastian O Siri:** Conceptualization, Methodology, Validation, Formal Analysis, Data Curation, Writing – Original Draft, Review and Editing
- **Victoria Rozés-Salvador**: Conceptualization, Methodology, Validation, Formal Analysis, Writing – Review and Editing
- **Emilce Artur de la Villarmois**: Electrophysiological experiments (Methodology, Validation and Formal Analysis)
- **Marisa S. Ghersi**: Electrophysiological experiments (Methodology, Validation and Formal Analysis)
- **Gonzalo Quassollo**: Technical and Imaging Assistance, Software
- **Mariela F. Pérez**: Validation, Formal Analysis of Electrophysiological experiments
- **Cecilia Conde**: Conceptualization, Investigation, Resources, Supervision, Project administration, Funding acquisition, Writing – Original Draft, Review and Editing, Visualization.

**Declaration of interests**

☒ The authors declare that they have no known competing financial interests or personal relationships that could have appeared to influence the work reported in this paper.

☐The authors declare the following financial interests/personal relationships which may be considered as potential competing interests:

**Highlights**

-Differential and dynamic distribution of recycling endosomes Rab11 in neurons

-Rab11 participates in the proper branching of the dendritic tree

-Rab11 is necessary for specific delivery of proteins to the somatodendritic domain

-LTP and spatial memory are abolished after Rab11 knockdown *in vivo*.

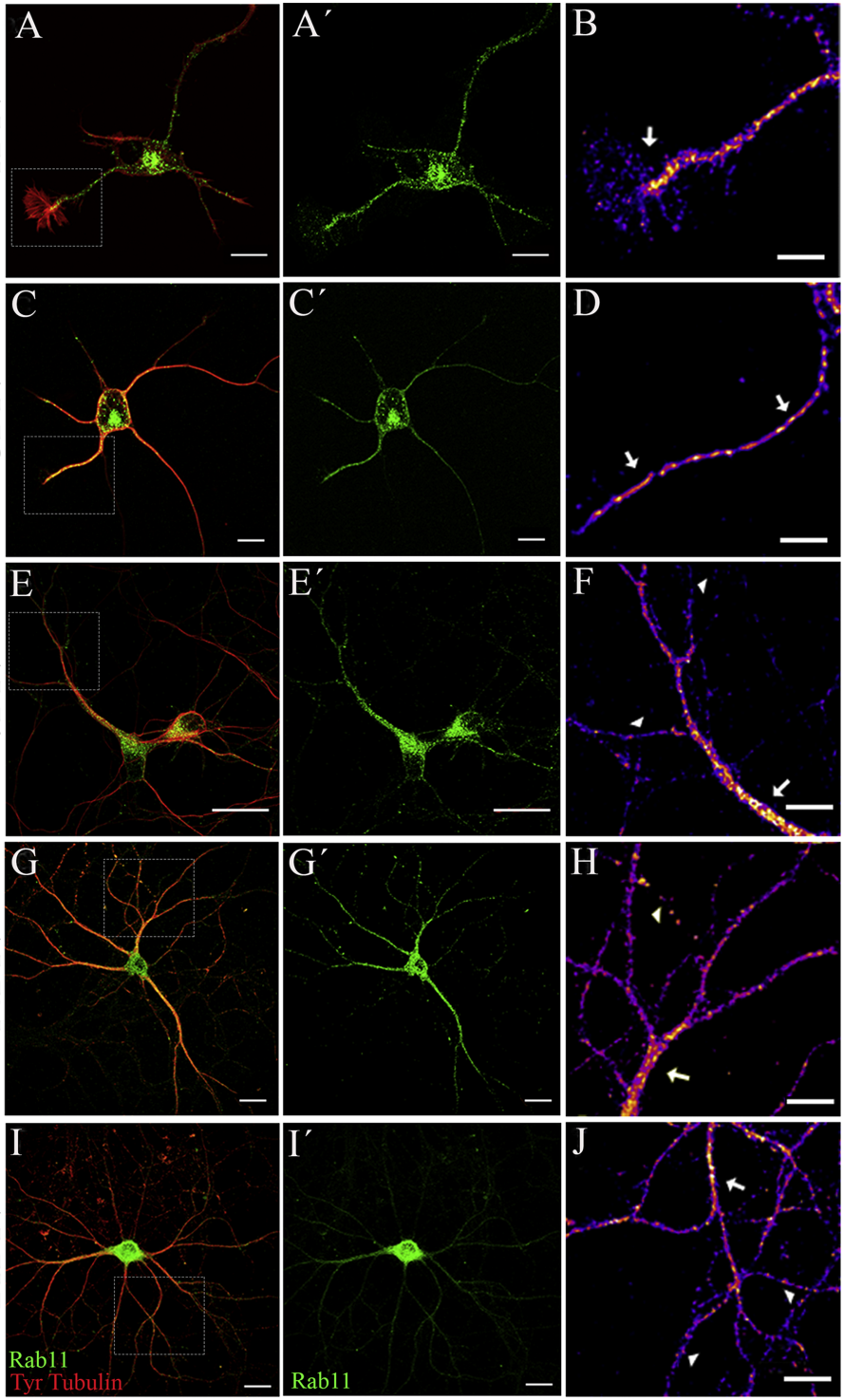
A
A´
B
1DIV
C
C´
D
3DIV
E
E´
F
7DIV
G
G´
H
14DIV
I
I´
J
21DIV
Rab11
Tyr Tubulin
Rab11

K

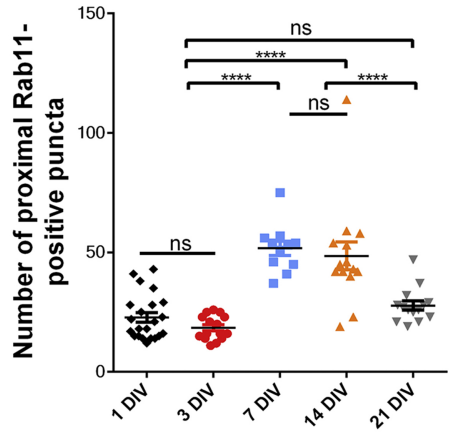
Number of proximal Rab11-positive puncta
150
100
50
0
ns
****
****
ns
****
ns
1 DIV
3 DIV
7 DIV
14 DIV
21 DIV

L

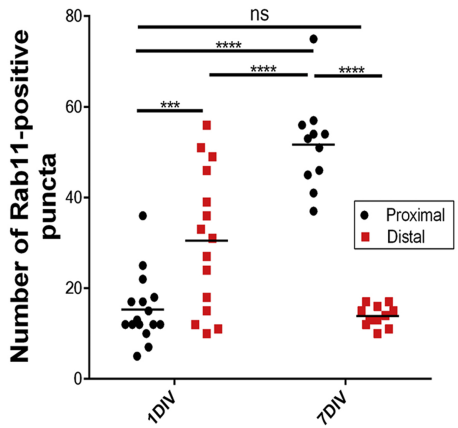
Number of Rab11-positive puncta
80
60
40
20
0
ns
****
****
****
***
Proximal
Distal
1DIV
7DIV

Figure 1

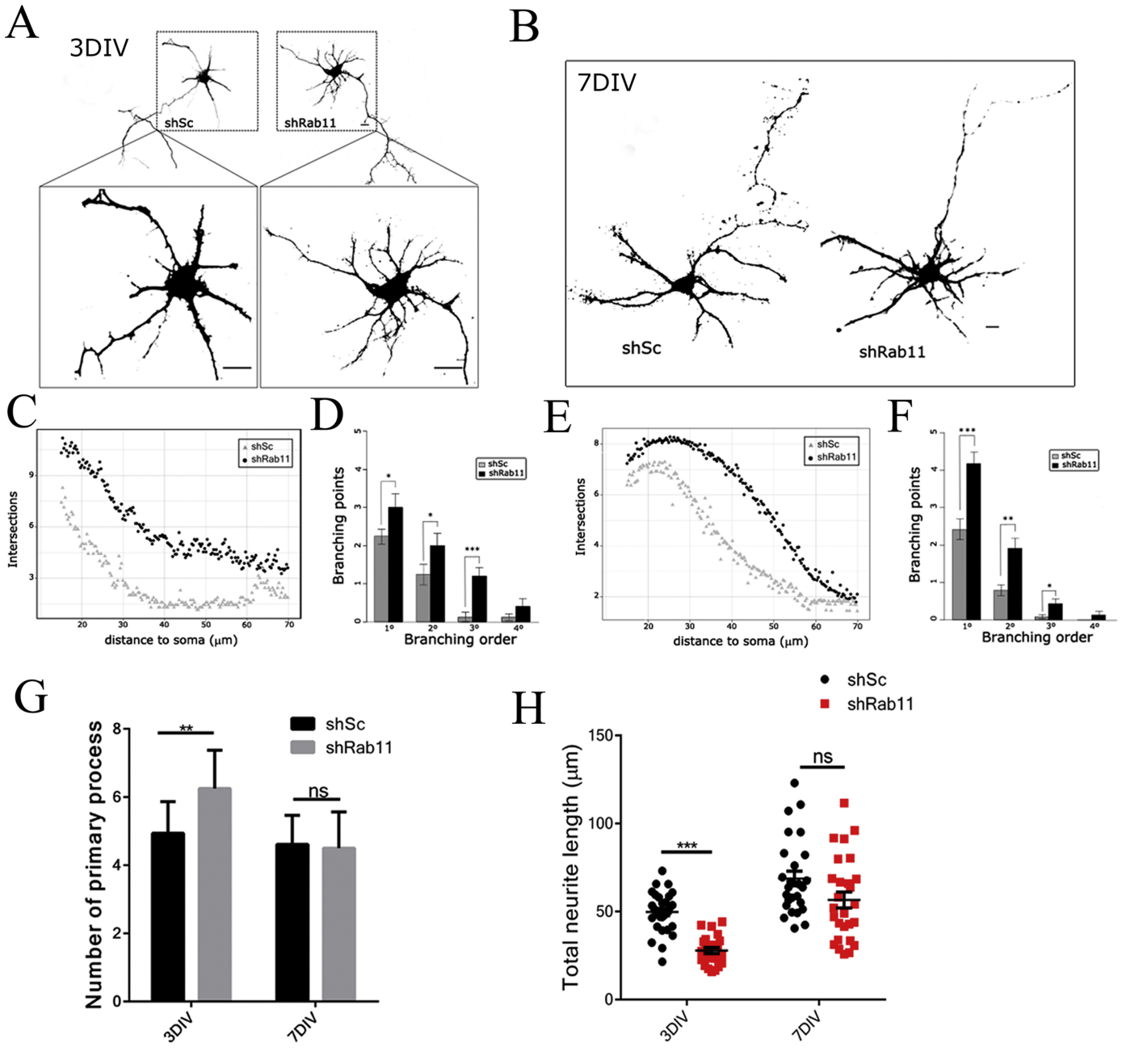
A
3DIV
shSc
shRab11
B
7DIV
shSc
shRab11
C
Intersections
distance to soma (μm)
shSc
shRab11
D
Branching points
Branching order
shSc
shRab11
E
Intersections
distance to soma (μm)
shSc
shRab11
F
Branching points
Branching order
shSc
shRab11
G
Number of primary process
shSc
shRab11
**
ns
3DIV
7DIV
H
shSc
shRab11
Total neurite length (μm)
***
ns
3DIV
7DIV

Figure 2

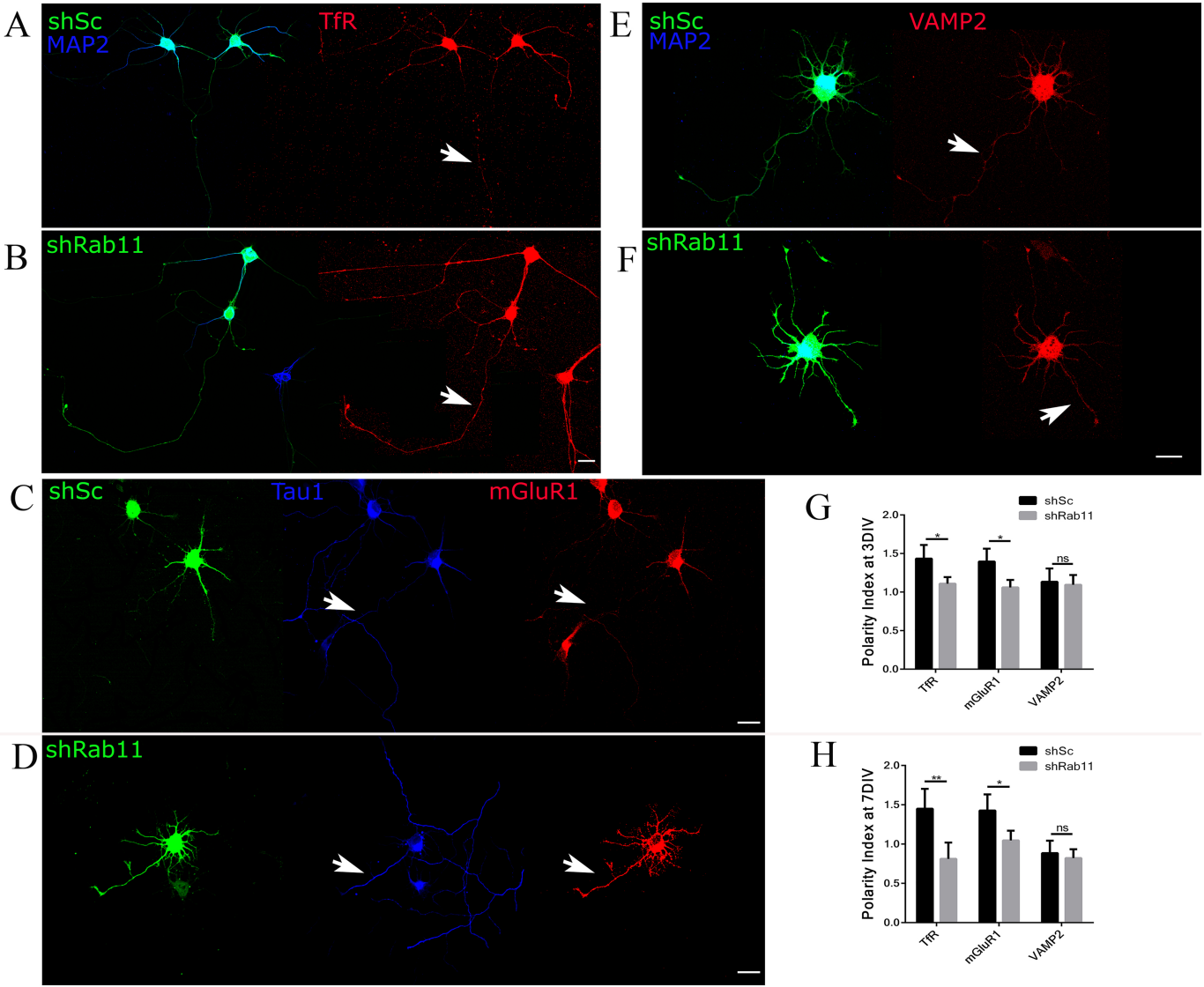
A
shSc
MAP2
TfR
B
shRab11
E
shSc
MAP2
VAMP2
F
shRab11
C
shSc
Tau1
mGluR1
D
shRab11
G
shSc
shRab11
Polarity Index at 3DIV
2.0
1.5
1.0
0.5
0.0
*
*
ns
TfR
mGluR1
VAMP2
H
shSc
shRab11
Polarity Index at 7DIV
2.0
1.5
1.0
0.5
0.0
**
*
ns
TfR
mGluR1
VAMP2

Figure 3

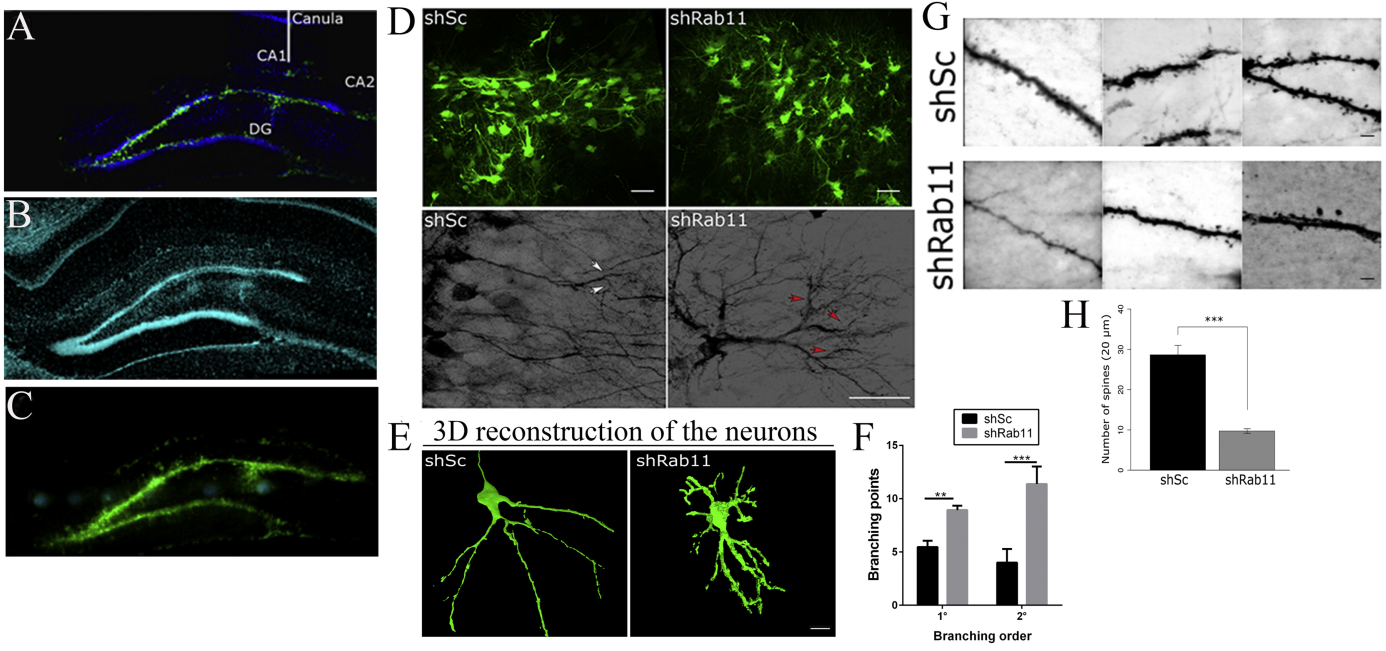
A
Canula
CA1
CA2
DG
B
C
D
shSc
shRab11
shSc
shRab11
E
3D reconstruction of the neurons
shSc
shRab11
F
shSc
shRab11
Branching points
Branching order
1°
2°
**
***
G
shSc
shRab11
H
Number of spines (20 µm)
shSc
shRab11
***

Figure 4

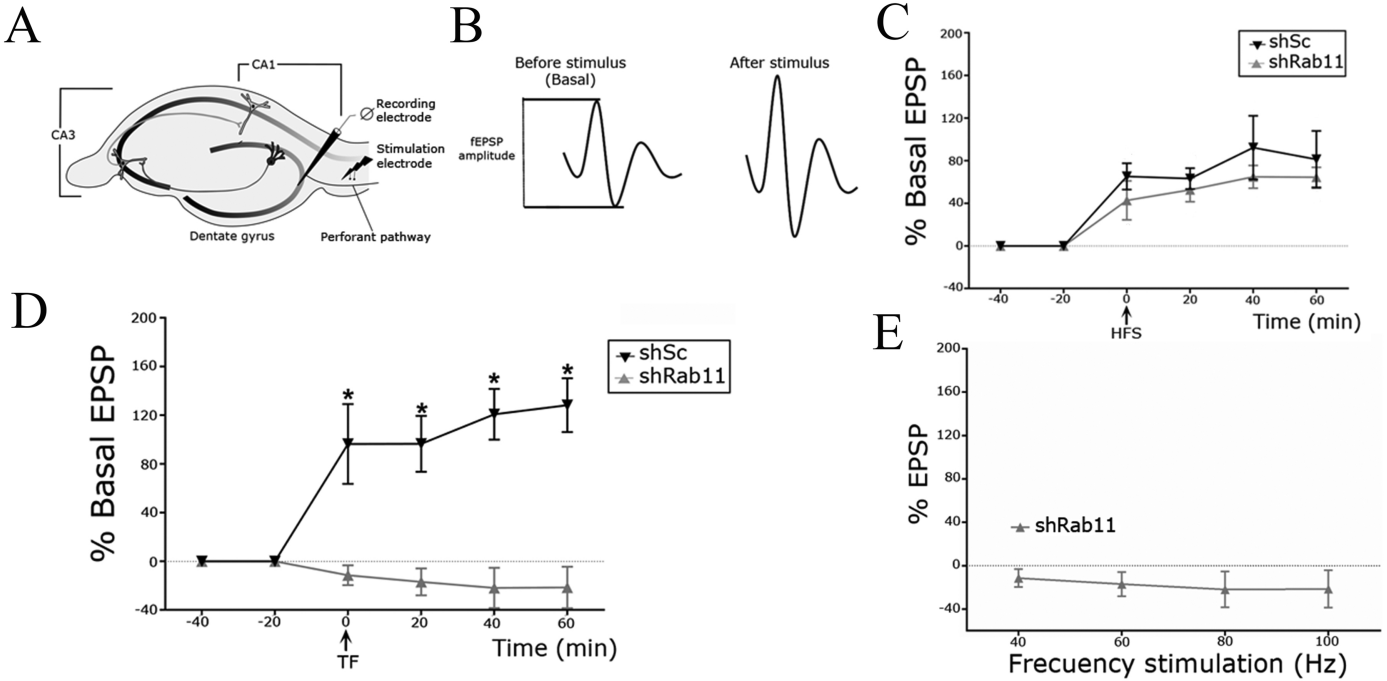
A
CA1
CA3
Recording electrode
Stimulation electrode
Dentate gyrus
Perforant pathway
B
Before stimulus (Basal)
After stimulus
fEPSP amplitude
C
shSc
shRab11
% Basal EPSP
HFS
Time (min)
D
shSc
shRab11
% Basal EPSP
TF
Time (min)
E
shRab11
% EPSP
Frecuency stimulation (Hz)

Figure 5

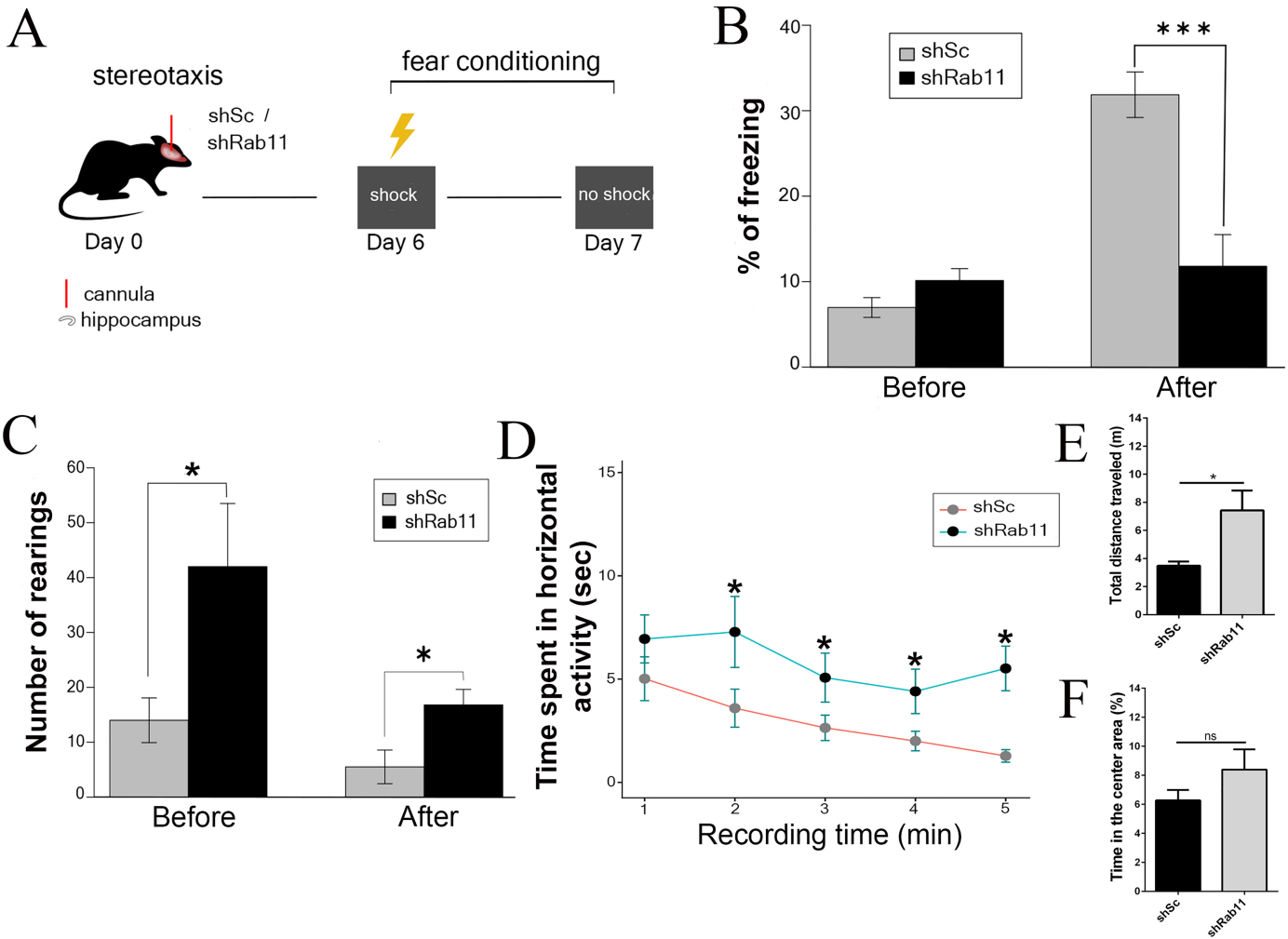
A
stereotaxis
shSc /
shRab11
fear conditioning
shock
no shock
Day 0
Day 6
Day 7
cannula
hippocampus
B
shSc
shRab11
***
% of freezing
Before
After
C
Number of rearings
shSc
shRab11
*
*
Before
After
D
Time spent in horizontal activity (sec)
shSc
shRab11
Recording time (min)
E
Total distance traveled (m)
*
shSc
shRab11
F
Time in the center area (%)
ns
shSc
shRab11

Figure 6

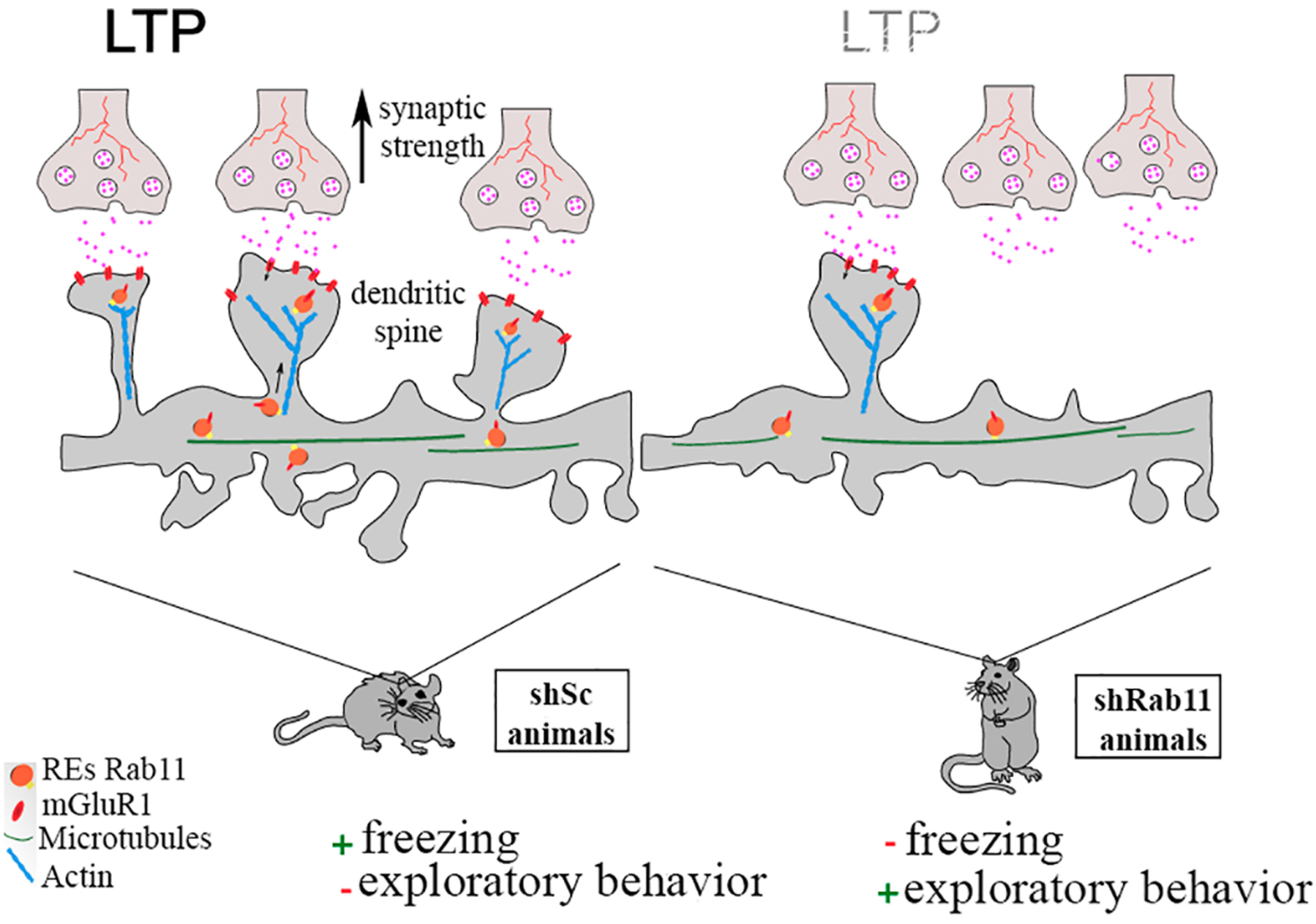
LTP
LTP
synaptic strength
dendritic spine
shSc animals
shRab11 animals
REs Rab11
mGluR1
Microtubules
Actin
+ freezing
- exploratory behavior
- freezing
+ exploratory behavior

Figure 7